

STRUCTURE OF STARS AND NUCLEI

Jürgen Schaffner-Bielich

Institut für Theoretische Physik, J. W. Goethe Universität, D-60054 Frankfurt am Main, Germany

Abstract In these lectures, the properties of dense hadronic and quark matter and its relation to compact stars will be discussed. In a bottom–up approach we start with nuclear and hypernuclear physics at low density and extrapolate hadronic matter to large densities. The matching to the quark matter phase is performed in a top–down approach starting at asymptotically large densities. Implications for the mass–radius relation of compact stars and the existence of a new family of solutions will be outlined.

1. Introduction: Elementary Matter and Neutron Stars

Neutron stars are created by supernovae type II explosions and are the final endpoint of evolution of massive stars. The compact remnants of the core collapse supernovae have masses in the range of 1–2 solar masses and radii of the order of 10 km. The interior of neutron stars consists of matter under extreme densities, several times the density of normal nuclear matter, $n_0 = 3 \cdot 10^{14} \text{ g/cm}^3$. The study of neutron stars has considerably advanced during the last years. With new telescopes, ground-based and in satellites, one measures spectra of supernova remnants like the crab nebula not only in the optical but also in the x-ray (Chandra, XMM–Newton), in radio as well as in the infrared band. The Hubble Space Telescope and the Chandra Telescope has even published a movie of the crab nebula on–line! These movies demonstrate how the rotating neutron star, the crab pulsar, pushes out energetic wisps into the crab nebula in the equatorial plane as well as jets of matter along the polar axis.

More than 1000 pulsars are known today. The masses of pulsars were measured most precisely from a few binary neutron star systems [1], especially from the Hulse–Taylor pulsar with $M = (1.4411 \pm 0.00035)M_\odot$. The shortest known rotation period so far measured is 1.557 ms for the pulsar PSR 1937+21.

Our knowledge about compact stars got a new twist by the discovery of isolated, non-pulsating neutron stars. The first one seen and the closest one known is RX J1856 [2] being radio-quiet and with no pulsations. The thermal spectrum indicates a temperature of 49 eV in the optical band. The x-ray spectrum, however, shows a nice Planck curve with a temperature of 60 eV

as measured by the Chandra satellite [3]. Most surprisingly, no spectral lines from elements in the atmosphere of the neutron star have been found in the spectra! These puzzles of the spectra of the isolated neutron star are still not fully resolved (see [4] for a possible explanations). The revised and improved parallax measurement of RX J1856 gives a distance of $D = 117 \pm 12$ parsec [5]. An ideal black-body emitter would have a very small radius of $R_\infty = 4 - 8$ km at that distance which is much smaller than the canonical value for a neutron star of 10 km [3]. Corrections from an atmosphere resulted in an apparent radius of $R_\infty = 15 \pm 3$ km which would be compatible with most of the modern neutron star models on the market [5, 6].

The structure of neutron stars encompasses several distinctly different zones when going from the surface to the centre (for a review see e.g. [7]). First, there is a thin atmosphere up to about 10^4 g/cm³, mainly iron but could be also hydrogen or helium by accretion. Then the outer crusts or the envelope begins which consists of free electrons and nuclei forming a Coulomb lattice. The sequence of nuclei starts with iron and then continues to neutron-rich nuclei stopping at the neutron drip-line at about 10^{11} g/cm³ [8]. The inner crusts consists of free neutrons in addition to nuclei and electrons where the neutrons are in a superfluid state. The nuclei can now form the pasta in the crust, various inhomogeneous phase structures as bubbles (meat-balls), rods (spaghetti), and plates (lasagna) immersed in the neutron and electron fluid. The sequence can then reverse, so that the neutron fluid forms the geometrical structures immersed in a background of extremely neutron-rich and superheavy nuclei [9].

At about half times normal nuclear matter density, the matter distribution will be uniform, consisting of mainly neutrons with a small admixture of protons and electrons, where the protons can now form a superconductor. Still, the end of the crust is located far away from the centre, as the crust is only a few hundred meters thick for massive neutron stars!

The core of the neutron star consists of matter under extreme densities. New forms of matter have been proposed to exist under these condition in the very core of compact stars: Bose condensation of pions or kaons, phase transitions to hyperon matter (hyperon star) and quark matter (hybrid star). If strange quark matter is absolutely stable, then the corresponding compact star is dubbed a strange star and the quark phase extends all the way from the centre to the neutron-drip line, as all free neutrons are swallowed by the true ground state of matter, while nuclei are saved by virtue of the Coulomb barrier.

Now let us start with a simple consideration: let us assume that the high-density equation of state can be described by free (known) particles. The stable baryons known in vacuum are the nucleons (n,p) and hyperons (the Λ and $\Sigma^{-,0,+}$ with one strange quark, the $\Xi^{-,0}$ with two strange quarks, and the Ω^- with three strange quarks). The masses of the hyperons increases with the number of strange quarks. Besides those, there are spinless mesons which are stable

against strong interactions (charged pions, and kaons with one anti-strange or one strange quark). They can form a Bose condensate. A calculation of neutron star matter for a free gas of particles shows, that first the negatively charged Σ^- appears at about $4n_0$ and then the Λ at about $8n_0$ [10]. The Σ^- appears before the Λ despite the fact that it is slightly heavier, because it is negatively charged. The presence of the Σ^- can then take over the rôle of the electron in making the overall matter charge neutral, thereby lowering the Fermi energy of electrons and the total energy of the system. One can compute that there will be no other particles in the composition of a free gas of hadrons up to $20n_0$ which is well beyond the maximum density in the interior of a compact star (besides that our approach will be not applicable anymore, as hadrons are composite particles). The corresponding equation of state will be even slightly softer than that of a free neutron gas due to the appearance of additional particles. Hence, the maximum mass is the one given by Oppenheimer and Volkoff for a free gas of neutrons which is about $0.7M_\odot$ [11]. That maximum mass is more than a factor two smaller than required by the measurement of the mass of the Hulse-Taylor pulsar of $1.44M_\odot$! Neutron stars can *not* be described by a approximately free gas of particles, contrary to white dwarfs. Interactions between hadrons are crucial for explaining such a large neutron star mass.

2. Nuclei with baryons: hypernuclei and strange hadronic matter

As hyperons seem to appear in dense hadronic matter relevant for compact stars, we study in the following the interactions between baryons of the baryon octet (nucleons, Λ , Σ 's, and Ξ 's) in dense matter. The nucleon-nucleon interaction is very well known from nuclear properties (the general problem is, of course, how to extrapolate the interaction to densities beyond normal nuclear matter density). For hyperons the situation is far less clear but a lot of information can be gathered from hypernuclear data and hyperonic atoms (for reviews see e.g. [12, 13]). Most of the hyperon-nucleon and hyperon-hyperon interaction known experimentally indicates an attractive potential.

The measured single particle levels of Λ hypernuclei from mass numbers of $A = 3$ to 209 result in a potential of $U_\Lambda = -30$ MeV at n_0 (see e.g. [14, 15]). It is well known, that the ΛN interaction gets repulsive at densities of about $2n_0$ and above [14, 16], so this nonlinear behaviour with density has to be taken into account for the modelling of neutron star matter.

For Σ 's, there is only one bound Σ hypernucleus known, $^4_\Sigma\text{He}$, which is, however, bound by isospin forces. Σ^- atomic data indicates a repulsive potential at n_0 [17] assuming again a nonlinear density dependence of the optical potential. This finding is consistent with the absence of narrow Σ hypernuclear

states (even in the continuum) for the reaction ${}^9\text{Be}(K^-, \pi^-)$ as measured at BNL [18].

There are seven Ξ hypernuclear events reported in the literature, which are summarised in [19]. Correcting the Ξ vacuum masses for the older events, one arrives at a relativistic potential of about -28 MeV at n_0 which is comparable to that of the Λ . However, more recent indirect estimates of the ΞN interaction by final state interactions in the reaction (K^-, K^+) on ${}^{12}\text{C}$ point towards a reduced attraction of about -14 MeV [20].

Double Λ hypernuclear states have been also seen experimentally (see [13] for a summary). Besides the three older candidates, there are two new measurements reported in 2001. Experiment E906 at BNL finds indications of about 400 produced ${}^4_{\Lambda\Lambda}\text{H}$ on a ${}^9\text{Be}$ target by the correlated emission of pions of the sequential weak decays. Experiment E373 at KEK reconstructs the production of a ${}^6_{\Lambda\Lambda}\text{He}$ and its subsequent weak mesonic decays. There are difficulties to reconcile the old and the new data in detail, but the overall consensus is that the $\Lambda\Lambda$ interaction must be attractive (see the discussion in [13]).

Note, that all other hyperon-hyperon interactions, as $\Lambda\Sigma$, $\Sigma\Sigma$, $\Lambda\Xi$, $\Sigma\Xi$, and $\Xi\Xi$ are essentially unknown experimentally!

The hyperon-hyperon interaction strength can be also probed by two particle correlations of e.g. two Λ s in relativistic heavy-ion collisions as it was measured recently by the NA49 collaboration [21]. Unfortunately, the statistics does not allow for a definite conclusion about the size of the s-wave scattering length of two Λ s, although the data indicates a small scattering length. As a lot of hyperons are produced in a single central heavy-ion collision at relativistic bombarding energies, multiply strange nuclear systems can be produced in the laboratory [22–25]. Indeed, the hypernuclei ${}^3_{\Lambda}\text{H}$ and ${}^4_{\Lambda}\text{H}$ can be seen in the invariant mass spectra of the weak decay products of Helium and a π^- [26].

Building up more and more hyperons in a "nucleus", the total binding energy of the system increases, as new degrees of freedom are filled up with a lower Fermi energy than nucleons. However, in the multi-hyperonic medium new reaction channels are possible, as $\Xi^- + p \rightarrow 2\Lambda$ and $\Xi^0 + n \rightarrow 2\Lambda$. These reactions are Pauli-blocked, as the possible lowest lying Λ hyperon states are filled up by Λ 's. Hence, the whole multi-hyperonic nucleus can be stabilised by virtue of the Pauli-blocking in the hyperon world! Relativistic shell model calculations find that the binding energy can be -13 MeV/A or even -21 MeV/A, depending on the strength of the hyperon-hyperon interactions [23, 24, 27]. Even purely hyperonic "nuclei", consisting of only Λ , Ξ^0 , and Ξ^- hyperons can exist with up to -8 MeV/A binding energy. More importantly, the charge of these systems is negative, while the baryon number is positive — indeed, a quite unusual nuclear property.

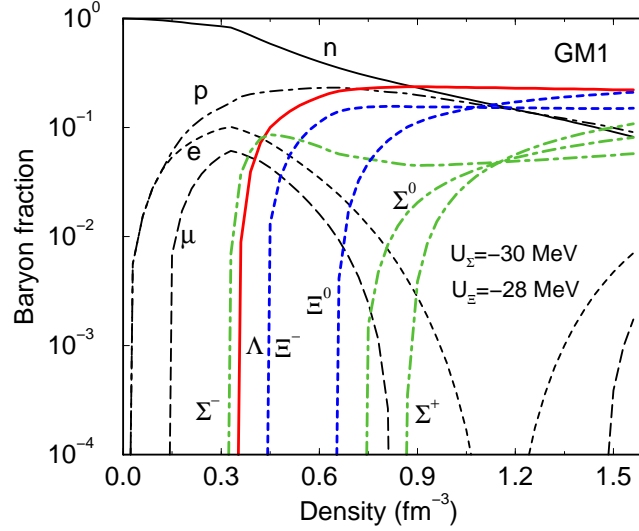


Figure 1. The composition of neutron star matter with hyperons within the relativistic mean-field model using parameter set 1 of [37] and an attractive potential for the Σ hyperons at n_0 .

3. Neutron Stars with baryons

As outlined in the introduction, hyperons will appear within a free gas of hadrons but interactions have to be taken into account to be compatible with the observed neutron star masses. Our more or less profound knowledge about the nucleon-nucleon, nucleon-hyperon, and hyperon-hyperon, the latter being the least well known of all, can be utilised to derive models for neutron star matter. In many different approaches emerges that hyperons, either the Λ or the Σ^- , appear in neutron star matter at about $2n_0$: in relativistic mean-field models [28–30], in a nonrelativistic potential model [31], in the quark-meson coupling model [32], in relativistic Hartree–Fock models [33], in Brueckner–Hartree–Fock calculations [34, 35], and within chiral effective Lagrangians [36]. Nevertheless, as we will show in the following, the details of the hyperon composition of neutron star matter is rather sensitive to the chosen hyperon potentials.

Fig. 1 shows the composition of neutron star matter as a function of density. At low densities, neutrons are dominating and there is a rapid rise of the proton and electron fraction. At about $2n_0$, first the Σ^- appears closely followed by the Λ . The electron fraction starts to drop at that density. At $3n_0$, the Ξ^- is present in neutron star matter before the lighter hyperons Σ^0 and the Σ^+ appear by virtue of its negative charge. The hyperon fraction considerably rises with increasing density. At $6n_0$ the Λ fraction even exceeds that of the neutron, being then the most populated baryon in matter in β equilibrium (which may more

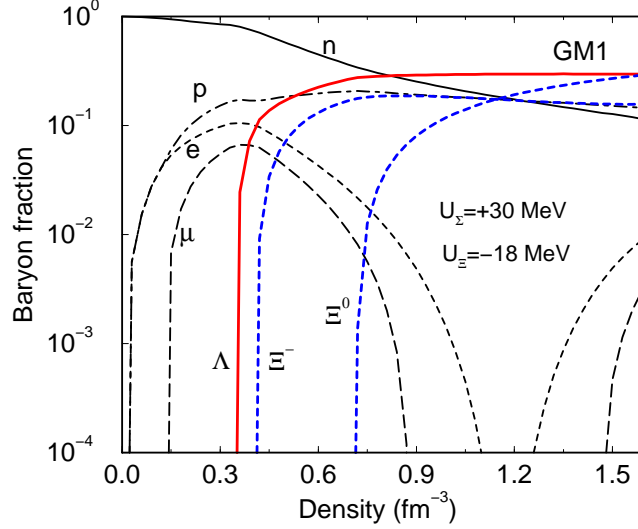


Figure 2. The composition of neutron star matter with hyperons, but now with a repulsive potential for the Σ hyperons at n_0 .

aply be called hyperon star matter). Neutron stars are giant multi-hypernuclei [28]! Note, that at about $7n_0$, electrons disappear and the isospin partners have equal fractions, as the isospin potential is negligibly small at these densities. At that point, the negatively charged Ξ^- balances the positive charge of the protons! At even larger densities, the matter distribution approaches about equal fractions for all baryons and positrons can be present. The positrons can not annihilate as there are no more electrons in the system left. The overall effect of the presence of additional degrees of freedom in the composition of a neutron star, be it hyperons or any other particle, is to lower the pressure and therefore to soften the equation of state. The maximum allowed mass for a neutron star will then decrease, typically from say $2M_\odot$ for a purely nucleonic star to about $1.5M_\odot$ for a hyperonic star depending on the parameter set used for the nucleon–nucleon interaction.

Now what happens if one just change the hyperon potentials, in particular switch the sign of the potential of the Σ hyperons from attraction to repulsion. Note that one adjusts the coupling constant of the Σ hyperons to the scalar meson slightly so as to get a repulsive potential at n_0 . All hyperon potentials are repulsive above, say $2n_0$, as pointed out above, due to the nonlinear density dependence of the baryon potentials. Furthermore, it is interesting to know, that the baryon potentials are dominated by its coupling to the vector mesons at large densities which are unaltered as their coupling strengths are fixed solely by symmetry constraints (SU(6) symmetry). Fig. 2 depicts the matter composition

for a repulsive potential of the Σ (at n_0) as indicated by Σ^- atomic data and a reduced attraction for the Ξ as extracted from final state interactions of Ξ s with ^{12}C . Here, a relativistic potential depth of $U_{\Xi} = -18$ MeV is taken, which is slightly larger than the non-relativistic one. The Σ hyperons are not present at all up to $10n_0$, demonstrating how a small change in the parameters can drastically shift its critical density. The only hyperons appearing in matter are the Λ , Ξ^- , and the Ξ^0 , in that order. Nevertheless, the onset of the Ξ^- population is shifted slightly towards lower densities to $2.5n_0$ compared to Fig. 1. The Ξ^- takes over the rôle of the Σ^- to diminish the fraction of electrons and its presence is even more favoured, if the Σ^- hyperons are absent. The Ξ hyperons constitute now a substantial fraction of the whole composition of hyperon star matter. Note, that the electron fraction starts to drop even before the critical density for the Ξ^- is reached. Once the neutral Λ fraction rises, the system lowers its energy by replacing protons with Λ s, thereby reducing again the Fermi energy of electrons which are needed to balance the charge of the protons. One might think, that a repulsive potential for the Ξ would also remove them completely from the matter distribution as the Σ s. However, this is not the case, the Ξ^- still appears, now at $3n_0$. The underlying reason is, that the repulsive vector potential for the Ξ s is a factor of two smaller than for the other hyperons and a factor three smaller than for nucleons as demanded by SU(6) symmetry for the vector coupling constants. The repulsive contribution to the overall potential, the vector potential, has to dominate at large densities to avoid a collapse of matter. Hence, the Ξ is more favoured than every other baryon at large densities due to its decreased repulsive potential and less sensitive to the changes of the hyperon potential at n_0 than the Σ .

So far we have not discussed the interactions between hyperons. As indicated by the scarce double hypernuclear data, the $\Lambda\Lambda$ interaction is attractive, maybe even more than the Λ -nucleon interaction. There is definitely an additional attractive contribution between two Λ s in nuclei, as the binding energy of two Λ s is more than just twice the binding energy of a single Λ . So additional potentials between hyperons have to be considered. Here we follow the discussion in [24, 30, 38]. It is natural to assume that there is scalar and a vector potential only between hyperons, as for nucleons and the nucleon-hyperon interaction. Utilising SU(3) symmetry arguments for the meson exchanges, the additional potentials appear to be just mediated by the missing members of the scalar and vector meson nonet: a hidden strange scalar meson, the $f_0(980)$, which we denote as σ^* in the following, and the hidden strange vector meson $\phi(1020)$. The vector coupling constant to the ϕ -meson can be fixed by SU(6) symmetry, so that all vector coupling constants are given in terms of the nucleon one. In SU(6) symmetry, there is ideal mixing between the singlet and octet states and the vector coupling constants are proportional to the number of light or strange quarks of the baryon, respectively. The conserved nonstrange vector current is

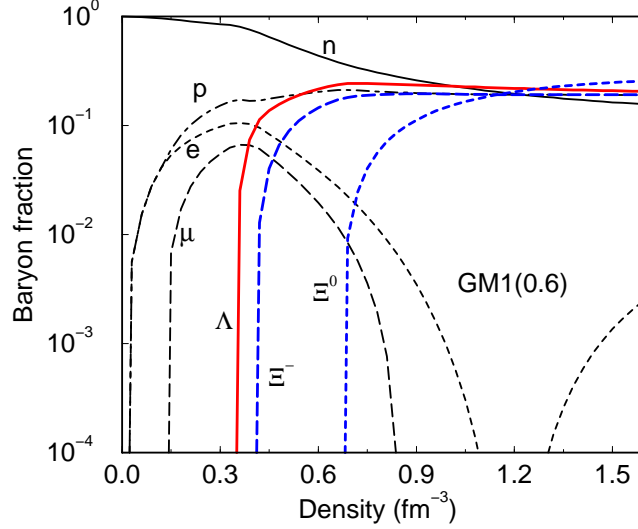


Figure 3. The composition of neutron star matter with hyperons including effects from an explicit hyperon–hyperon interaction ($g_{\sigma^*\Lambda}/g_{\sigma N} = 0.6$).

then proportional to the light quark number current, while the hidden strange vector current is proportional to the strange quark number current. The scalar meson coupling constant to the σ^* will be adjusted to the hyperon–hyperon interaction strength. We assume that the σ^* meson coupling constants scale with the number of strange quarks, like for the ϕ meson coupling constants. As a consequence of these arguments, the hyperon–hyperon interaction between Ξ s should then be twice as strong as between Λ s and Σ s. The overall strength of the hyperon–hyperon interaction is then controlled by one parameter, the hidden strange scalar coupling constant of the Λ to σ^* .

Fig. 3 shows the composition, if the additional potentials for the hyperon–hyperon interaction are taken into account with $g_{\sigma^*\Lambda}/g_{\sigma N} = 0.6$. As one can see, there is not a substantial change in the composition of neutron star matter compared to the case without explicit hyperon–hyperon interactions. The appearance of hyperons is hardly modified. One notices, however, that the hyperon fraction at large densities is reduced, so that the hyperon fraction does not exceed the neutron fraction anymore. The composition at large densities is now uniform, there are about equal amounts of all baryons present (except for the Σ hyperons). The reduced fraction of hyperons at large densities is due to the additional vector potential between hyperons which dominates over the attractive hidden strange scalar potential at large hyperon densities. The equal abundance of all baryons, except for the Σ s, is due to the fact that the sum of vector potentials of each baryon scales with the total number of quarks, not

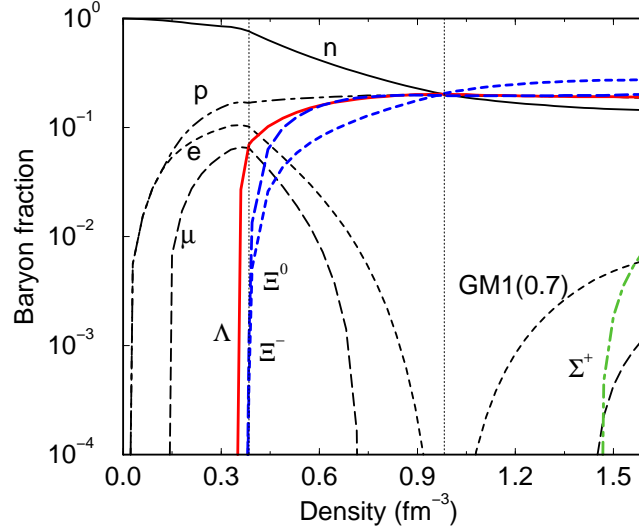


Figure 4. The composition of neutron star matter with hyperons, now for a slightly increased hyperon–hyperon interaction ($g_{\sigma^*\Lambda}/g_{\sigma N} = 0.7$). A first order phase transition appears, the boundaries of the mixed phase are marked by the vertical dotted lines.

with the number of light quarks. The strange twist by including the attractive hyperon–hyperon interaction is that the hyperon fractions are reduced. The hyperon–hyperon interaction is attractive at normal nuclear density and for a small hyperon population, but it turns repulsive for a large hyperon density i.e. in the core of a neutron star. The additional repulsions helps to stabilise the system at large densities in the sense that the equation of state gets stiffer at large densities.

Now let us increase the strength of the hyperon–hyperon interaction slightly from $g_{\sigma^*\Lambda}/g_{\sigma N} = 0.6$ to $g_{\sigma^*\Lambda}/g_{\sigma N} = 0.7$. Fig. 4 depicts the composition of neutron star matter. Surprisingly, the composition has drastically changed. The Λ population sets in slightly before the appearance of the Ξ hyperons, which appear together at about $2.5n_0$. At $6.5n_0$, the baryon fractions are equal to each other and the electrons, as well as the muons, have disappeared in the medium. A first order phase transition from nucleon dominated to hyperon dominated hadronic matter appeared in the neutron star matter at $2.5n_0$! Using the general Gibbs criterion to model the phase transition (see e.g. [39]), the electron fraction is continuous through the boundaries of the mixed phase. Negatively charged bubbles of hyperon dominated matter form which are immersed in slightly positively charged nucleon dominated matter. At the end of the mixed phase at $6.5n_0$, the situation is reversed, now positively charged bubbles of nucleon dominated matter is present in the background of slightly negatively charged

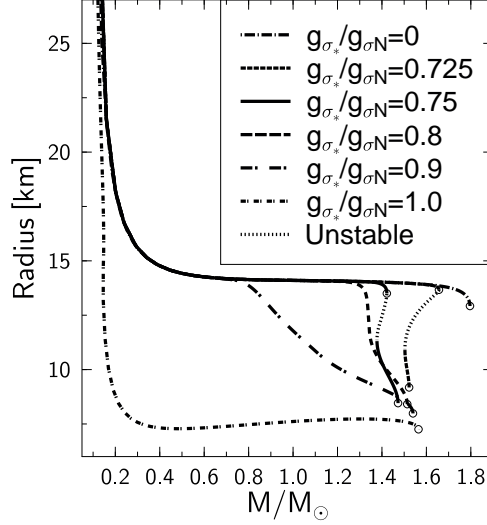


Figure 5. The mass–radius relation of compact stars for different interaction strengths of the hyperon–hyperon potential. For increasing hyperon–hyperon attraction, the radius of the maximum mass compact star decreases down to only $R = 7 - 8$ km. In some intermediate cases, an additional branch of stable solutions appears (taken from [38]).

hyperon dominated matter. At each stage, the criterion of total global (not local) charge neutrality is fulfilled. The boundaries of the mixed phase are marked by the vertical dotted lines in the figure. Note that the mixed phase extends over a quite large region of density, thereby constituting a substantial fraction of the total matter inside a neutron star. Geometrical phases appear in the mixed phase, bubbles, rods and slabs, like in the liquid–gas phase transition of nuclear matter in the crust. The charged structures will form a Coulomb lattice, thereby changing the liquid to a solid and modifying the transport properties of the inner parts of a neutron star.

The presence of a first order phase transition in neutron star matter has also an important impact on the global properties of compact stars [38]. The mass–radius relation for compact stars is shown in Fig. 5 for different hyperon–hyperon interaction strengths. For a moderate hyperon–hyperon interaction strength, $g_{\sigma^*\Lambda}/g_{\sigma N} = 0.725$ and 0.75 , the maximum mass is reduced while the corresponding radius is unaltered in the ordinary neutron star branch. In addition, there appears a new branch of solutions at smaller radii but similar (maximum) masses. The dotted lines denote the unstable regions of the solution, where the compact star is unstable with respect to radial oscillations. The dashed and full lines then indicate that the solution is stable against radial oscillations, as the mass increases with decreasing radii. The maximum mass of this new

branch of solution amounts to about $1.5M_{\odot}$ with a radius of about only 7–8 km. The compact stars representing this new family of solutions are hypercompact stars. For comparison, the maximum mass of the ordinary neutron star branch lies at similar values while the radius is much larger, around 13 km. Note, that hypercompact stars can have larger or lower masses than the maximum mass of the ordinary neutron star branch.

Increasing the hyperon–hyperon interaction, the new family of solution disappears and there is a continuous stable line in the mass–radius diagram. The maximum mass compact star is, however, now always located close to the hypercompact star branch, i.e. at about $1.5M_{\odot}$ with a radius of about 7–8 km. A new effect happens for the case $g_{\sigma^*\Lambda}/g_{\sigma N} = 1.0$. For asymptotically large radii, that means for low densities, the mass and radius is like in the other cases. The masses of the compact stars stay, however, below $0.2M_{\odot}$ down to radii of 7–8 km and increase with a rather constant radius up to a maximum mass of about $1.6M_{\odot}$. The underlying equation of state for this case is one which exhibits a vanishing pressure at a finite value of the energy density, a feature characteristic for absolutely stable matter, like absolutely stable strange quark matter [40, 41]. The corresponding compact stars are so called selfbound, as they are stabilised by strongly attractive interactions, contrary to ordinary compact stars which are hold together by the gravitational force. The outermost layer of material of a selfbound compact star consists of the same material as for the outer crust of an ordinary neutron star: a lattice of nuclei in a sea of electrons. The maximum density of that crust must be below the neutron drip density, as free neutrons will be eaten up by the absolutely stable matter which is more deeply bound than ordinary matter. Nuclei survive due to the Coulomb barrier between them and the phase of absolutely stable matter. There is a strong jump in baryon density, accompanied by a similar jump in the electron density which constitutes the Coulomb barrier, of three orders of magnitude at the phase boundary of nuclear matter and absolutely stable matter. As the crust material is the same for selfbound stars and neutron stars, the mass-radius curves approach each other for low central energy densities and large radii, where most of the material is residing in the crust. The properties of selfbound strange hadronic matter are similar to the ones of selfbound strange quark matter [42, 43].

Let us come back to the issue of the new branch of stable solutions. Fig. 6 demonstrates the general feature of the mass–radius relation for compact stars. For white dwarfs, the mass increases for decreasing radii up to the Chandrasekhar mass, the maximum mass of white dwarfs. Beyond that limiting mass, the solutions are unstable against radial oscillations, until the mass increases again for decreasing radii. The family of neutron stars has been reached now, which is again stable up to some maximum mass which depends sensitively on the hadronic interactions. Beyond that maximum mass for neutron stars, the mass–radius relation curves either in a (unstable) spiral down to some

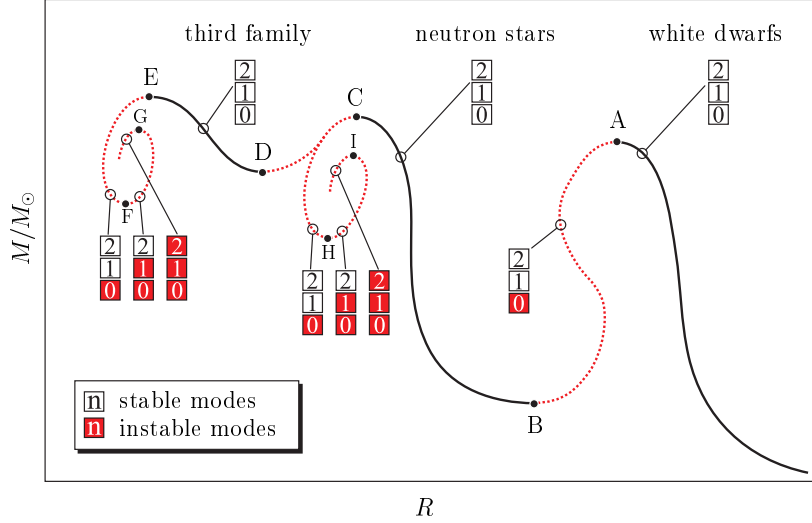


Figure 6. A sketch of the mass–radius relation of compact stars. The curves with an increasing mass while lowering the radius are stable solutions. A third solution can appear for radii below the ones for ordinary neutron stars (taken from [44]).

fixed point or continues again to increase the mass with lower radii. The latter case is stable against radial oscillations and marks the onset of a new family of stable solution of compact stars. The masses of these new branch can have similar values as those of ordinary neutron stars, so that they can be dubbed neutron star twins, but the radii are considerably smaller. After the maximum mass of the third family is reached, the unstable final spiral appears which marks the end of Tolman–Oppenheimer–Volkoff (TOV) solutions for hadronic matter.

The existence of a new family of compact stars besides white dwarfs and ordinary neutron stars stems from the presence of a strong first order phase transition in the equation of state. The input for the TOV equations is just the macroscopic relation between energy density and pressure. The microscopical details are not relevant for the global properties of compact stars. Hence, the first order phase transition can be to anything, like to strange quark matter in hybrid stars [45, 44, 46], to a pion condensed phase [47], to a kaon condensed phase [48], or, as discussed above, to strange hadronic matter [38]. The criterion for the existence of a new branch in the mass–radius relation of compact stars has already been discussed by Gerlach in 1968 [49]. The new branch appears to be stable, if the equation of state changes rapidly from a rather soft one to a much harder one. Exactly this feature is present at the end of the mixed phase of a strong first order phase transition, no matter what the underlying reason for that strong phase transition is.

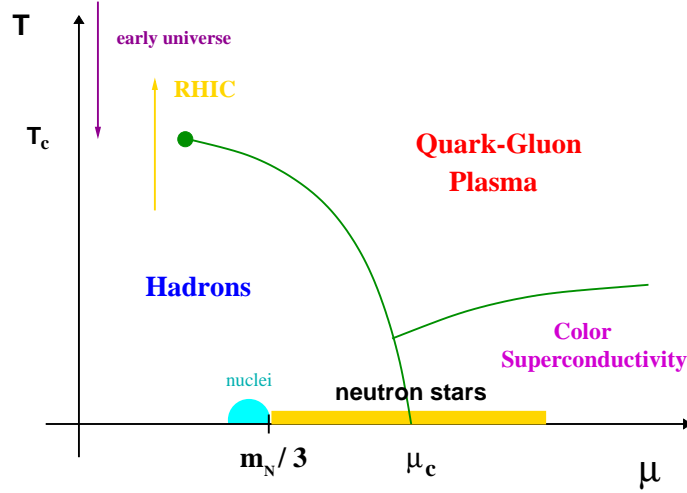


Figure 7. The phase diagram of QCD for finite temperature and quark chemical potentials. There is a line of a first order phase transition starting at zero temperature and a critical quark chemical potential μ_c and stopping in a critical endpoint where the phase transition is of second order (taken from [51]).

4. Neutron stars with quarks

In the previous section, we started with some interaction fixed to properties of matter at low densities, that means at n_0 , which is a bottom-up approach for the description of dense, cold matter. In this section, we want to discuss the issue of the strong first order phase transition in terms of a top-down approach. At sufficiently large densities, the more appropriate description of dense matter will be in terms of quarks, which are, according to our present understanding of QCD, asymptotically free.

For large temperatures and vanishing net baryon density, lattice gauge simulations indicate, that the phase transition is first order for pure gluon theory and likely to be a rapid crossover at about $T_c = 170$ MeV in full QCD including dynamical quarks [50]. On the lattice, it was seen that when the quark condensate drops at T_c the Polyakov loop increases. The quark condensate is an order parameter for the chiral phase transition, where the quarks are getting massless for vanishing current quark masses for $T \geq T_\chi$. The Polyakov loop is an order parameter for pure gluon theory and has a nonvanishing value in the deconfined phase for $T \geq T_d$. Hence, the lattice data demonstrates that $T_c = T_\chi = T_d$ at zero quark-chemical potential. Why these two entirely different phase transitions happen at the same temperature is presently not fully understood. In principle, the chiral and the deconfinement phase transitions can happen at entirely different scales in QCD.

Neutron stars probe a very different region of the phase diagram of QCD (see Fig. 7). Neutron star matter is cold on nuclear scales and has an extremely large baryon density. At some critical value of the quark chemical potential μ_c , there is a first order phase transition to colour superconducting quark matter [52–55] which is based on theoretical arguments (see [56–59] for reviews about the many phases of QCD). Matter with colour superconducting quarks occupies the phase diagram at large chemical potentials and moderate temperatures. For large chemical potentials and temperatures, there will be a quark–gluon plasma. The line of first order phase transition which started at $T = 0$ and $\mu = \mu_c$ stops in a critical point. At that point the phase transition is of second order, beyond the point at larger temperatures the phase transition is a rapid crossover. The precise location of that critical endpoint is not known at present.

Recently, lattice simulations started to explore the phase diagram of QCD at finite quark chemical potential attempting to find the critical endpoint. The extension to finite μ is performed by reweighting techniques or a Taylor expansion which will fail, of course, if μ/T gets large. So far, first lattice calculations find values of about $\mu_{\text{end}} = 400 - 700$ MeV [60, 50]. In any case, it is quite likely that there is a first order phase transition at finite density and low temperature which is right in the region of interest for neutron star matter.

We now study the following picture of cold and dense matter: at low densities there are hadrons and at intermediate densities the description of dense matter will be more appropriate in terms of massive quarks. The transition from hadrons to massive quarks is assumed to be smooth. Then there is a phase transition from massive quarks to massless quarks at the chiral phase transition $\mu = \mu_\chi$. For $\mu > \mu_\chi$, perturbative QCD is used as a model of the equation of state of QCD and for $\mu < \mu_\chi$ a matching to the low density equation of state has to be performed [46, 59]. The thermodynamic potential can be computed up to order α_s^2 for massless quarks from which all thermodynamic observables are derived self-consistently (pressure, energy density, and baryon number density). The renormalisation subtraction point needs to be fixed in the perturbative treatment. It should be proportional to the overall scale of the system and is chosen to be $\bar{\Lambda}/\mu = 2, 3$. One finds then, that the resulting pressure starts at some finite value of the chemical potential and approaches very slowly the Stefan–Boltzmann limit of a free gas. Even at rather large densities, say of $n = 30n_0$, there are still sizable corrections to a simple free gas of quarks.

The matching to the low density equation of state can happen basically in two ways: either the matching appears to be smoothly from the low to the high density part or the matching incorporates a drastic change of the slope of the pressure as a function of chemical potential. Fig. 8 depicts the situation schematically. If the pressure in the low density equation of state increases rapidly with density, the matching will be smooth and the phase transition is weakly first order. On the other hand, if the pressure rises slowly with density

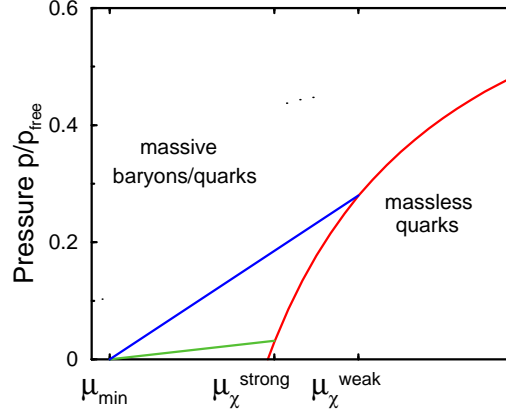


Figure 8. The matching of the low density equation of state to the high density matter of massless quarks (taken from [51]). Depending on the rise of the pressure in the low density phase, the matching results in a weak phase transition at μ_{weak} (upper line) or a strong phase transition at μ_{strong} (lower line).

the phase transition will be strongly first order. Now the matching of the two equation of states results in a significant change of the slope of the curves in Fig. 8. As the slope reflects just the number density, the baryon density as well as the energy density will jump at the matching point causing a strong first order phase transition. Which situation is realized in nature, is not clear. Nonrelativistic model calculations of asymmetric matter [61] hint at that the pressure in the low density regime stays small up to about $2n_0$, being only a few percent of that of a free gas of quarks, so that a strong first order phase transition is not excluded a priori.

Fig. 9 shows the mass–radius relation for various equation of states. The solid lines stand for pure quarks stars calculated in perturbative QCD, the long–dashed ones are calculated within the MIT bag model, a free gas of massless quarks only modified by a constant bag pressure. The curves for quark stars start at zero mass and radius as the pressure vanishes at a finite energy density — no hadronic mantle has been taken into account which would change the mass–radius relation at small masses to large radii (see e.g. the discussion of Fig. 5). The mass–radius relation for a purely hadronic equation of state is depicted on the right side of the plot. At some chosen critical density, the phase transition to quark matter occurs. The corresponding hybrid stars have smaller radii. For $n_c = 2.5n_0$, a new family of stable solution appears where the short–dashed line turns into a solid line. The matching is done for the quark matter equation of state producing quark stars with a rather low mass of only $1M_\odot$ and a corresponding radius of only 6 km. Depending on the matching of the hadronic to the quark matter equation of state, the new family of solution lies

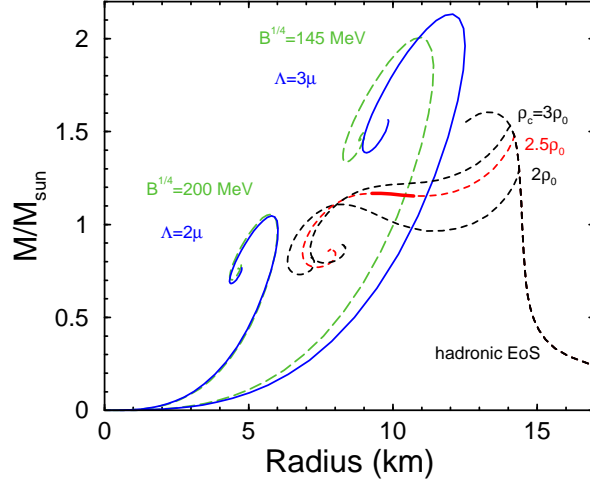


Figure 9. The mass radius relation of pure quark stars are shown by the solid lines (perturbative QCD) and long-dashed lines (MIT bag model). The mass-radius curves for a hadronic equation of state (EoS) with a phase transition to quark matter are plotted with short-dashed lines for different critical densities. A new stable solution appears where the curve turns from a short-dashed to a solid line.

somewhere between the curves for pure hadronic and pure quark stars, i.e. radii down to 6 km are in principle possible for the new family of compact stars. We note in passing, that there is a recent flurry of activity studying effects from color superconducting quark matter on the mass-radius relation of compact stars [62–68].

It is clear from the previous discussion, that the studies of compact stars is far from being completed. Further investigations of the nonperturbative treatments of the quark phase and how it matches to the low density equation of state are needed to elucidate the possible existence of a new family of compact stars. The recent data from present x-ray satellites, Chandra and XMM Newton, and the Hubble Space telescope have considerably advanced our knowledge of the properties of compact stars with more surprising news to come. Future telescopes, like the x-ray satellite XEUS and the Next Generation Space Telescope, are poised to finally pin down the mass-radius relation of compact stars and to determine the equation of state of cold and dense, strongly interacting matter. Excitingly, this means also that the possible existence of hypercompact stars might be confirmed within the coming years!

Acknowledgments

It is a pleasure to thank Eduardo Fraga, Norman Glendenning, Matthias Hanauske, Rob Pisarski, and Igor Mishustin with whom I collaborated on the

topics addressed in these lectures and Mark Alford for comments. I am indebted to Walter Greiner and Horst Stöcker for their continuous support which made this work possible. I especially thank Walter Greiner for inviting me to give these lectures.

References

- [1] S. E. Thorsett and D. Chakrabarty, *Astrophys. J.* **512**, 288 (1999).
- [2] F. M. Walter, *Astrophys. J.* **549**, 433 (2001).
- [3] J. J. Drake *et al.*, *Astrophys. J.* **572**, 996 (2002).
- [4] V. Burwitz *et al.*, *Astron. Astrophys.* **399**, 1109 (2003).
- [5] F. M. Walter and J. Lattimer, *Astrophys. J.* **576**, L145 (2002).
- [6] J. A. Pons *et al.*, *Astrophys. J.* **564**, 981 (2002).
- [7] P. Haensel, EAS Publications Series, volume 7, Final Stages of Stellar Evolution, Proceedings of the conference held 16-21 September, 2001 in Aussois, France, edited by C. Motch and J.-M. Hameury, p. 249 (2003).
- [8] G. Baym, C. Pethick, and P. Sutherland, *Astrophys. J.* **170**, 299 (1971).
- [9] J. W. Negele and D. Vautherin, *Nucl. Phys.* **A207**, 298 (1973).
- [10] V. A. Ambartsumyan and G. S. Saakyan, *Sov. Astron.* **4**, 187 (1960).
- [11] J. R. Oppenheimer and G. M. Volkoff, *Phys. Rev.* **55**, 374 (1939).
- [12] C. J. Batty, E. Friedman, and A. Gal, *Phys. Rep.* **287**, 385 (1997).
- [13] A. Gal, *Nucl. Phys.* **A721**, 945 (2003).
- [14] D. J. Millener, C. B. Dover, and A. Gal, *Phys. Rev. C* **38**, 2700 (1988).
- [15] M. Rufa *et al.*, *Phys. Rev. C* **42**, 2469 (1990).
- [16] J. Schaffner-Bielich, I. N. Mishustin, and J. Bondorf, *Nucl. Phys.* **A625**, 325 (1997).
- [17] J. Mares, E. Friedman, A. Gal, and B. K. Jennings, *Nucl. Phys.* **A594**, 311 (1995).
- [18] S. Bart *et al.*, *Phys. Rev. Lett.* **83**, 5238 (1999).
- [19] C. B. Dover and A. Gal, *Ann. Phys. (N.Y.)* **146**, 309 (1983).
- [20] P. Khaustov *et al.*, *Phys. Rev. C* **61**, 054603 (2000).
- [21] C. Blume *et al.*, *Nucl. Phys.* **A715**, 55 (2003).
- [22] J. Schaffner, C. Greiner, and H. Stöcker, *Phys. Rev. C* **46**, 322 (1992).
- [23] J. Schaffner *et al.*, *Phys. Rev. Lett.* **71**, 1328 (1993).
- [24] J. Schaffner *et al.*, *Ann. Phys. (N.Y.)* **235**, 35 (1994).
- [25] J. Schaffner-Bielich, R. Mattiello, and H. Sorge, *Phys. Rev. Lett.* **84**, 4305 (2000).
- [26] L. E. Finch *et al.* (E864 collaboration), *Nucl. Phys.* **A661**, 395c (1999).
- [27] J. Schaffner-Bielich and A. Gal, *Phys. Rev. C* **62**, 034311 (2000).
- [28] N. K. Glendenning, *Astrophys. J.* **293**, 470 (1985).
- [29] R. Knorren, M. Prakash, and P. J. Ellis, *Phys. Rev. C* **52**, 3470 (1995).
- [30] J. Schaffner and I. N. Mishustin, *Phys. Rev. C* **53**, 1416 (1996).
- [31] S. Balberg and A. Gal, *Nucl. Phys.* **A625**, 435 (1997).
- [32] S. Pal *et al.*, *Phys. Rev. C* **60**, 015802 (1999).

- [33] H. Huber, F. Weber, M. K. Weigel, and C. Schaab, *Int. J. Mod. Phys.* **E7**, 301 (1998).
- [34] M. Baldo, G. F. Burgio, and H. J. Schulze, *Phys. Rev. C* **61**, 055801 (2000).
- [35] I. Vidana *et al.*, *Phys. Rev. C* **62**, 035801 (2000).
- [36] M. Hanauske *et al.*, *Astrophys. J.* **537**, 958 (2000).
- [37] N. K. Glendenning and S. A. Moszkowski, *Phys. Rev. Lett.* **67**, 2414 (1991).
- [38] J. Schaffner-Bielich, M. Hanauske, H. Stöcker, and W. Greiner, *Phys. Rev. Lett.* **89**, 171101 (2002).
- [39] N. K. Glendenning, *Phys. Rev. D* **46**, 1274 (1992).
- [40] E. Witten, *Phys. Rev. D* **30**, 272 (1984).
- [41] E. Farhi and R. L. Jaffe, *Phys. Rev. D* **30**, 2379 (1984).
- [42] P. Haensel, J. L. Zdunik, and R. Schaeffer, *Astron. Astrophys.* **160**, 121 (1986).
- [43] C. Alcock, E. Farhi, and A. Olinto, *Astrophys. J.* **310**, 261 (1986).
- [44] K. Schertler, C. Greiner, J. Schaffner-Bielich, and M. H. Thoma, *Nucl. Phys.* **A677**, 463 (2000).
- [45] N. K. Glendenning and C. Kettner, *Astron. Astrophys.* **353**, L9 (2000).
- [46] E. S. Fraga, R. D. Pisarski, and J. Schaffner-Bielich, *Phys. Rev. D* **63**, 121702(R) (2001).
- [47] B. Kämpfer, *J. Phys. A* **14**, L471 (1981).
- [48] S. Banik and D. Bandyopadhyay, *Phys. Rev. C* **64**, 055805 (2001).
- [49] U. H. Gerlach, *Phys. Rev.* **172**, 1325 (1968).
- [50] F. Karsch, *hep-lat/0401031* (2004).
- [51] E. S. Fraga, Y. Hatta, R. D. Pisarski, and J. Schaffner-Bielich, *nucl-th/0301062* (2003).
- [52] B. C. Barrois, *Nucl. Phys. B* **129**, 390 (1977).
- [53] D. Bailin and A. Love, *Phys. Rep.* **107**, 325 (1984).
- [54] M. Alford, K. Rajagopal, and F. Wilczek, *Phys. Lett. B* **422**, 247 (1998).
- [55] R. Rapp, T. Schäfer, E. V. Shuryak, and M. Velkovsky, *Phys. Rev. Lett.* **81**, 53 (1998).
- [56] K. Rajagopal and F. Wilczek, *hep-ph/0011333* (2000).
- [57] T. Schäfer, *hep-ph/0304281* (2003).
- [58] D. H. Rischke, *Prog. Part. Nucl. Phys.* **52**, 197 (2004).
- [59] M. Alford, *nucl-th/0312007* (2003).
- [60] Z. Fodor and S. D. Katz, *JHEP* **03**, 014 (2002).
- [61] A. Akmal, V. R. Pandharipande, and D. G. Ravenhall, *Phys. Rev. C* **58**, 1804 (1998).
- [62] M. Alford and S. Reddy, *Phys. Rev. D* **67**, 074024 (2003).
- [63] M. Baldo *et al.*, *Phys. Lett. B* **562**, 153 (2003).
- [64] S. Banik and D. Bandyopadhyay, *Phys. Rev. D* **67**, 123003 (2003).
- [65] D. Blaschke *et al.*, *AIP Conf. Proc.* **660**, 209 (2003).
- [66] I. Shovkovy, M. Hanauske, and M. Huang, *Phys. Rev. D* **67**, 103004 (2003).
- [67] S. B. Rüster and D. H. Rischke, *Phys. Rev. D* **69**, 045011 (2004).
- [68] M. Buballa, F. Neumann, M. Oertel, and I. Shovkovy, *nucl-th/0312078* (2003).